Available online at www.sciencedirect.com

ScienceDirect

St. Petersburg Polytechnical University Journal: Physics and Mathematics 1 (2015) 47–55

www.elsevier.com/locate/spjpm

Field-induced electron emission from nanoporous carbon of various types

Alexander V. Arkhipov[a], Pavel G. Gabdullin[a], Nikolai M. Gnuchev[a,*], Sergei N. Davydov[a], Svyatoslav I. Krel[a], Boris A. Loginov[b]

[a] *St. Petersburg Polytechnic University, 29 Politekhnicheskaya St., St. Petersburg 195251, Russian Federation*

[b] *National Research University of Electronic Technology, 5 Pass. 4806, Zelenograd, Moscow 124498, Russian Federation*

Available online 12 March 2015

Abstract

The influence of fabrication technology on field electron emission properties of nanoporous carbon (NPC) has been investigated. Samples of NPC derived from different carbides via chlorination at different temperatures demonstrated similar low-field emission ability with the threshold electric field strength of 2–3 V/μm. This property correlated with the presence of nanopores with the characteristic size of 0.5–1.2 nm determining high values of specific surface area (more than 800 m^2/g) of the material. In most cases, voltage–current characteristics of emission were approximately linear in Fowler–Nordheim (FN) coordinates (excluding the low-current part near the emission threshold), but the plot slope angles were in notable disagreement with the known material morphology and electronic properties, and this could not be explained within the frames of FN emission theory. We suggest that the actual emission mechanism for NPC involves hot electrons generated at internal boundaries, and that emission centers may be associated with relatively large (20–100 nm) onion-like particles observed in many microscopy images.

Keywords: Nanoporous carbon; Field electron emission; Carbon nanomaterials; Graphite-like nanoparticles.

1. Introduction

During the recent decade, carbon-based field emitters developed into a promising option of cold cathodes for various devices [1,2]. Carbon nanotubes (CNTs) [3] were the first nanocarbon form that found practical applications in microwave [4,5], light [6] and X-ray [7,8] sources, plasma devices [9], space thrusters [10], microelectronic components [11,12] and gauges [13]. However, the fabrication processes of controlled CNT arrays remain relatively complex and expensive. Furthermore, the problem of their fast degradation under operational conditions has not yet been solved [3,7,14–16]. Due to the very high geometric aspect ratio, the CNTs provide substantial local amplification of the applied electric field which helps to achieve low-field emission. Yet the resulting concentration of the emission current, electric force, thermal load and ionic bombardment at atomic-scale areas eventually

* Corresponding author.
E-mail addresses: arkhipov@rphf.spbstu.ru (A.V. Arkhipov), pavel-gabdullin@yandex.ru (P.G. Gabdullin), gnuchev.nm@spbstu.ru, nmg@rphf.spbstu.ru (N.M. Gnuchev), phys-el@spbstu.ru (S.N. Davydov), 8svyatoslav8@mail.ru (S.I. Krel), logi@miee.ru (B.A. Loginov).

http://dx.doi.org/10.1016/j.spjpm.2015.03.011

(Peer review under responsibility of St. Petersburg Polytechnic University).

lead to accelerated destruction of the emission sites. This drawback of the CNT-based technologies stimulates involvement into emission investigations of alternative forms of nanocarbon, such as nanodiamond [17–27], nanographitic [2,26–28], amorphous [29–31] and composite [32–36] films. All these materials have common features of heterogeneous composition and (more or less) disordered structure. Their surface topography is relatively smooth, so that the estimated values of field enhancement factor β are insufficient to describe the observed low-field emission within the frame of the classical Fowler–Nordheim (FN) theory. A number of principally different models were developed to explain this phenomenon [24–26,31–33,37–40]. Most commonly, a proposed mechanism of emission facilitation involves a multistage tunnel transfer of electrons via nanosized domains with contrast electronic properties [2,18–20,41–47].

2. Samples: preparation, physical and chemical properties

In the present work, we investigated field-emission properties of nanoporous carbon (NPC) – one of all-carbon materials with disordered nano-scale structure. Similar materials were studied previously in Refs. [48,49], but in our work we used a particular form of NPC, produced from carbides through chlorination process [50–55] in which selective etching reaction had removed all non-carbon elements and formed a solid structure with high porosity. Due to developed pore/skeleton interface, homogeneity of pore size, strong adsorption ability, relatively high electric conductance and mechanical strength, the carbide-derived NPC materials give considerable promise for diverse applications, including fabrication of field electron emitters [56].

Detailed description of the process of NPC samples fabrication from the carbides of boron, zircon, titanium and molybdenum and typical parameters of the product structure were disclosed in [53–55]. The structural parameters substantially differed for the samples of different origin. Thus, the mean pore size for the products of B4C and Mo2C chlorination was approximately 5 times greater than that for ZrC and TiC derivatives. As a result, the apparent density in the latter case was almost two times greater, while the pycnometric density (i.e. the density of carbon skeleton, with pore volume excluded from consideration) was close to the density of graphite for all the samples.

Silicon carbide was also used for fabricating NPC samples for the described experiments. As it has been showed in [55], the pore size for these samples varied

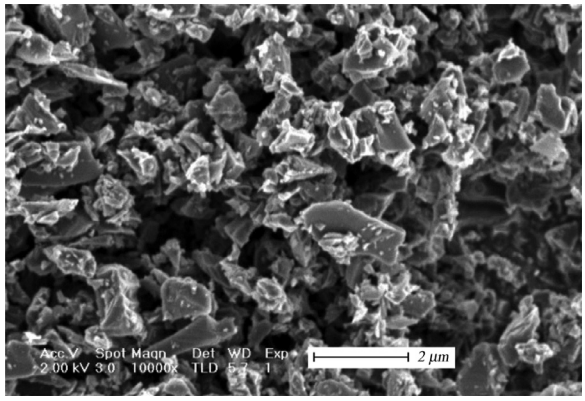

Fig. 1. A typical overview SEM image of an NPC sample (produced from SiC by chlorination at 1200 °C).

in wider range than for the derivatives of other carbides. Chlorination temperature had significant effect on the pore size distributions. In the samples prepared at low temperatures (700–900 °C), the pore size was close to 1 nm. If the chemical treatment temperature was higher (1200°), larger pores appeared and the sample densities (both apparent and pycnometric ones) decreased, presumably due to higher chlorine etching efficiency with respect to carbon atoms. After treatment at 2000 °C, only large pores (meso-pores) remained in the sample; the carbon skeleton lost more than a half of its mass and underwent a reconstruction with dramatic reduction of the specific surface area.

The morphology of the studied NPC samples may be overviewed from microscopic images. All overview images (with relatively low resolution and wide field of view) acquired with a scanning electron microscope were similar to the one presented in Fig. 1. The μm- and sub-μm-sized irregular NPC particles presented in the image inherit the shapes of the original carbide powder grains.

Atomic-scale images of small spots of NPC samples obtained by the transmission electron microscopy (HR TEM) are shown in Fig. 2a–c. They demonstrate that the studied materials included both amorphous (Fig. 2c) and ordered domains.

The latter were comprised of faceted (Fig. 2a) or curved (Fig. 2b) atomic layers. The distances between atomic planes (~0.35 nm) correspond to the graphite lattice period. Domain sizes between 20 and 100 nm were the most typical, though sometimes larger faceted crystallites were also observed (Fig. 2d). As much as it can be seen from microscopic data, the relative part of ordered domains in NPC samples derived from the same carbide usually grew with the increase of chlorination temperature [52,55].

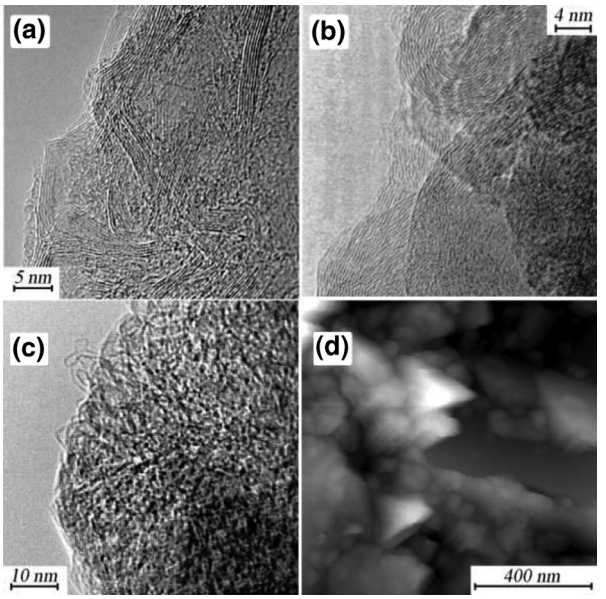

Fig. 2. Typical nm-scale morphological elements of NPC surface in HR TEM ((a)–(c)) and AFM (d) images.

3. Emission properties

Emission properties of NPCs were tested in the layout described previously in [56]. Emitter samples were prepared by depositing NPC powders over plane metal substrates. The electric field was applied between the sample and a cylindrical tungsten anode with a flat end side in vacuum better than 10^{-6} Torr. The field gap width between the anode and cathode was 0.50–0.75 mm, the anode diameter was 6 mm. During the experiments, the samples could be heated up to 400 °C to remove volatile contaminants and perform thermo-field activation procedures [56].

All the investigated NPC coatings demonstrated comparable emission properties. Emission characteristics of NPC samples fabricated from different carbides are compared in Fig. 3.

For all the presented plots, the threshold field values corresponding to the appearance of a minimum measurable (sub-nanoAmp) current are within the 2–3 V/μm range, which may be considered as the demonstration of high emission efficiency. Unfortunately, many samples of the same series, fabricated in the same technological process, demonstrated much worse emission properties. This witnesses certain instability of the used fabrication technology and/or that the emission characteristics were determined by some poorly controlled parameters of the samples.

The NPC samples produced from silicon carbide by chlorination at different temperatures also demonstrated similar emission properties (Fig. 4), excluding the case of the highest temperature of 2000 °C.

This special form of NPC with very low specific surface did not yield any emission current in the fields up to 10 V/μm.

The current dependencies measured in the emission tests usually demonstrated exponential character (for the field values well above the emission threshold): presented in FN coordinates (Figs. 3b and 4b), the emission plots were approximately linear. In accordance with the classical field-emission model, their slope angles are determined by the combined parameter ($\phi^{3/2}/\beta$), where ϕ is the work function of the emitter and β is the field enhancement factor for the emitting spot. For the presented plots, this parameter varied between 2.0×10^{-3} and 6.5×10^{-3} eV$^{3/2}$. Taking $\phi = 4.5$ eV as a typical value for various forms of carbon [28,38,57], we obtain an estimate for the field enhancement factor

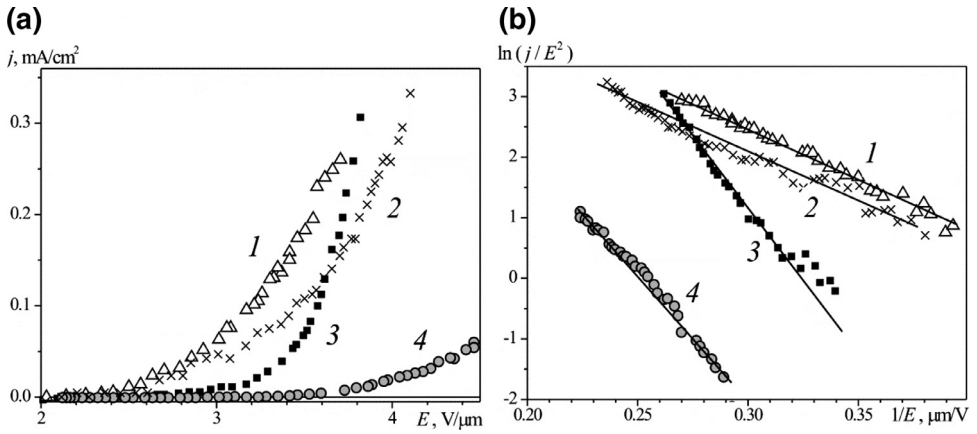

Fig. 3. Emission *I–V* plots in straight (a) and FN (b) coordinates for NPC samples fabricated from different carbides: TiC (1), Mo_2C (2), ZrC (3), B_4C (4).

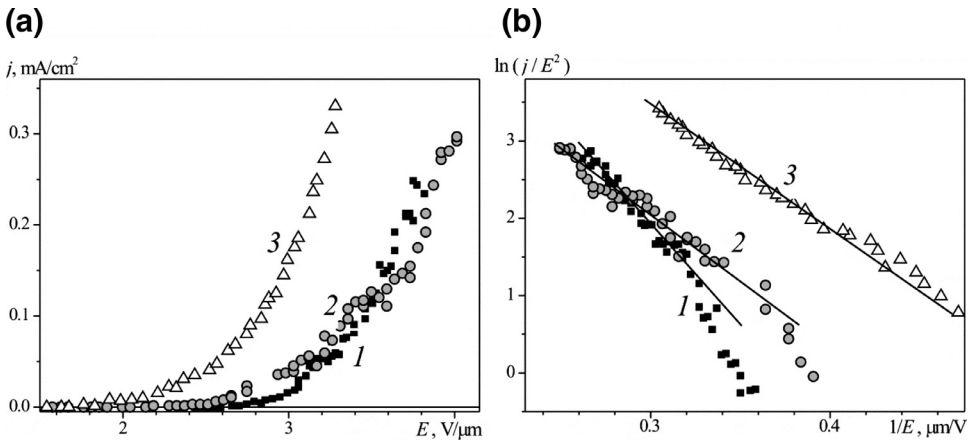

Fig. 4. Emission *I–V* plots in straight (a) and FN (b) coordinates for NPC samples fabricated from SiC by chlorination at different temperatures, °C: 700 (1), 900 (2), 1200 (3).

$\beta \approx 1500$–4500. These values obviously disagree with the surface topography revealed by the microscopic studies (see Figs. 1 and 2). A more plausible value $\beta = 10$ gives us the work function estimates of 0.07–0.16 eV. For a material with such a little work function, heating to 400 °C would result in thermal emission with space-charge-limited current density of more than 10 A/cm^2. No such emission current weakly depending on the applied field was ever observed in the experiments. Thus, we can conclude that the experimental data apparently disagree with the classical emission theory, which is not unusual for many forms of carbon.

Near the emission threshold, the disagreement between the measured current characteristics and theoretical predictions was often even more notable. Fig. 5 represents a few typical emission plots with the intervals of current saturation and even reduction.

Such features were most typical for the emission current values below 3–5 μA, but sometimes they were seen at much higher currents (Fig. 5b). High probability of their appearance does not allow explaining their existence through fluctuations of the current. The features were reproduced in multiple measurements in increasing and decreasing field, which also excludes a number of possible explanations, such as thermal effects or removal of contaminant layers.

The contradiction between the observed presence of the "fine structure" at low-current parts of the emission plots and smooth exponential growth at higher currents can be naturally explained by statistical averaging of the emission characteristics of local centers, individually having complicated shapes. Near the emission threshold, only a limited number of the most efficient centers contribute to the full current [58]. As the field increases, this number grows and individual features are averaged out.

Thus, the performed experiments with different varieties of NPC have demonstrated that the NPC can efficiently emit electrons in relatively weak electric field, if only they have a developed nm-scale structure characterized by large specific surface area of nanopores. Like for many other forms of nanocarbon, the phenomenon of low-field emission from NPC and some features of current characteristics cannot be adequately described by Fowler–Nordheim theory as well, so probably the mechanism of direct electron transfer to vacuum from the Fermi level of the emitter surface layer is irrelevant to this material.

4. Discussion

Some authors [58–60] associate the phenomenon of low-field emission from all the forms of nanocarbon with the enhancement of electric field at high-aspect-ratio elements (nanotubes, fibers, etc.), even when these elements are not introduced intentionally and are present at the emitter surface in relatively low numbers as a technological contaminant. Even though this explanation may be correct for some of the discussed emitters, we think that in the NPC materials investigated in this work, the emission mechanism is different. Besides the fact of low-field emission itself, the actual emission model for NPC has also to explain other experimentally observed features of the emission behavior, including:

- the reproducible "fine structure" of emission characteristics near the field threshold, discussed above;

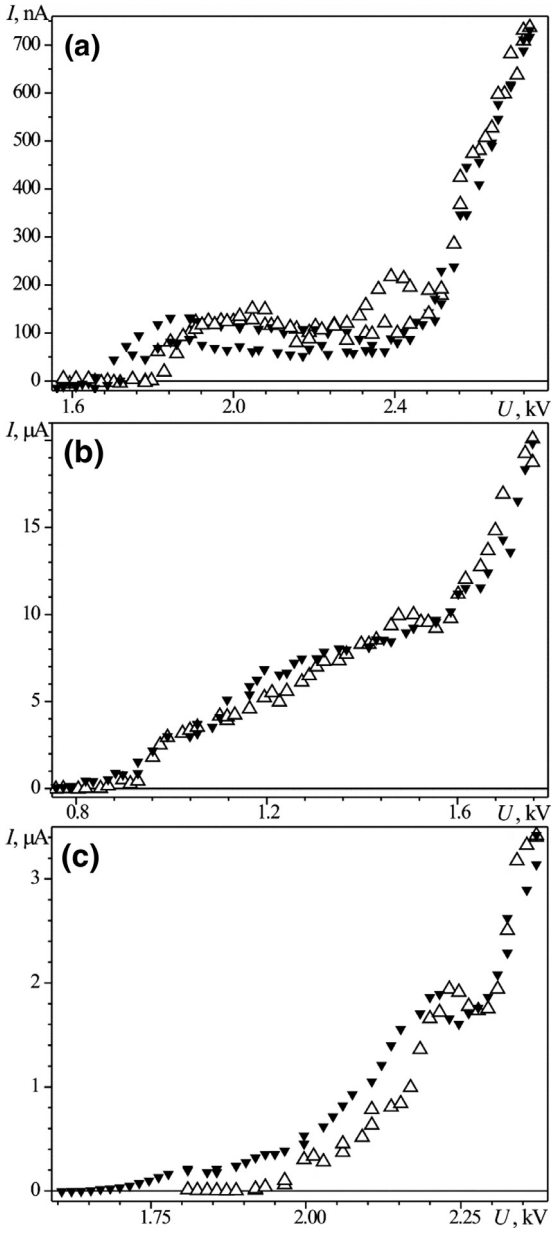

Fig. 5. Emission *I–V* plots for NPC samples with typical reproducible deviations from exponential shape, measured at different ranges of applied voltage. Date acquisition time was close to 1 min per curve. Empty and filled symbols mark the data measured with increased and decreased voltage, respectively.

- the hysteresis of emission from NPC in pulsed field (at sub-μs and even μs time scale) described in previous publications [61];
- relatively wide (up to 1 eV) energy distributions of the emitted electrons [62];
- the results of independent definition of the field enhancement factor ($\beta \approx 15$) and energy position of "emitting" electron states in NPC (electron affinity should be equal to $\chi_S \approx 0.3$–0.6 eV, i.e. much lower than the work function for carbon $\phi \approx 4.5$–5.0 eV), performed on the basis of the measured emission characteristics in pulsed field [63].

We assume that all these features of NPC emission may be explained in terms of the two-stage model of the emission mechanism [2,18–20,41–47] with a few important modifications discussed below. According to this model, electrons are transferred from the emitter bulk electron states near the Fermi level (E_F) to vacuum not directly, but through two successive steps via some intermediate states localized near the emitter surface, with energies substantially higher than E_F. If electrons are elevated onto such non-equilibrium states, they can be effectively emitted to vacuum because the surface potential barrier is lower in this case and more transparent for them than for the electrons at Fermi level. Yet, for the realization of this emission mechanism, taking into account the phenomena mentioned above, the following conditions must be satisfied:

(a) the applied electric field should penetrate into the emitter material to produce free energy that is necessary to elevate the electrons to high-energy states (i.e. to generate "hot" electrons);
(b) inside the emitter, the field should be concentrated at the internal boundaries to be able to provide some electrons with relatively large (eV-scale) additional energy;
(c) the hot electrons should be able to propagate to the vacuum boundary and remain there for a considerable time without thermalization.

The available information on the NPC structure and properties suggests that all the listed conditions may be satisfied.

According to [50–55] and our own microscopic data, the NPC is a porous conglomerate of small (1–2 nm) graphene sheets mixed with larger onion-like or graphitic-shelled particles, up to 50–200 nm in size. Electronic properties of the material are those of a *p*-type semiconductor [51], which means a non-zero band gap and Fermi level position near the valence band top. The excessive holes appear due to electron trapping at interface boundary states, and thus all the crystalline volumes are charged positively relative to their boundaries. Due to strong band bending, the nanodomains are separated from each other by tunnel junctions allowing external field to penetrate into the material. Polarization

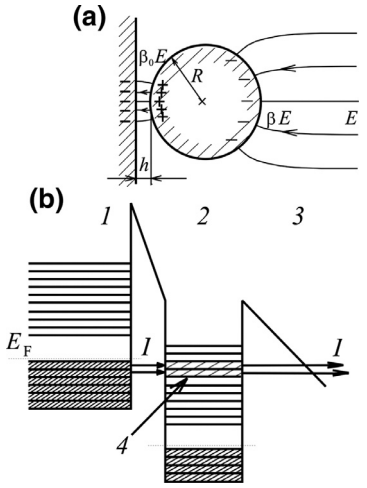

Fig. 6. The suggested structure of an active emission center on the NPC surface: schematic geometry (a) and energy diagram (b); 1 – emitter bulk, 2 – nanoparticle, 3 – vacuum, 4 – long-living hot electrons; R – radius of the nanoparticle, h – width of the gap between the particle and the conductive plane, E_F – Fermi level, I – emission current, E – external field strength; β, β_0 – coefficients of external and internal field enhancements.

of the domains leads to enhancement of the applied field at the junctions (Fig. 6).

The enhancement factor can be roughly estimated via the solution of an electrostatic problem considering a conductive sphere (the nanodomain) of radius R placed at a small distance h (junction) from a conductive plane (the rest of the emitter). In this system, the electric field E applied normally to the plane is locally enhanced by the factor $\beta_0 = AR/h$, where $A \approx 0.5$. For example, if the particle size is 80 nm and the junction width is 0.4 nm, the additional internal field enhancement can reach 100, which may be sufficient for our model. A similar problem was investigated in [64] for ellipsoidal sp^2 particles in an amorphous layer on a conductive substrate, and the enhancement factors up to 300 were considered. Potential difference between the adjacent domains can reach 1 V in the electric field with moderate magnitude of less than 10 V/μm, and the electrons injected through the interface junctions will have the energies much higher than the local Fermi level (Fig. 6).

However, to increase emission efficiency, these hot electrons have to reach the outer emitter boundary and to remain in its vicinity for a relatively long time without relaxation. According to recent studies [65,66], such possibility appears if the considered medium is composed by nanoparticles with the size of approximately 30 nm or smaller. The electron relaxation time dramatically increases (in comparison with larger crystallites) due to so-called "phonon bottleneck effect" [67–69] associated with reduced density of states in the conductance band of nanodomains, leaving energy gaps between adjacent levels exceeding maximum phonon energy for this lattice. Therefore, the most efficient mechanism of energy losses – the electron–phonon interaction – is practically excluded. The experiments performed in [70] confirm that mean recombination time for hot charge carriers may grow to 1 ns and higher. This is more than sufficient for the electrons which were injected from the "back" side of a surface-layer crystallite to propagate across the grain. If the relaxation is very slow, it can even explain the hysteresis of the characteristics of emission in pulsed field observed in the work [61].

So, all the conditions necessary for the enhanced electron emission may be fulfilled due to the presence of conductive nanoparticles in the structure of NPC materials. These particles are presumably capable to concentrate electric field at internal interfaces. This property "replaces" field enhancement at outer morphology elements of emitters based on nanotubes and fibers, and can be even preferable for the practical use – the region of concentrated field and current is protected from external impacts, such as ionic bombardment. On the surface where these factors are present, the field is less concentrated, which can result in higher emitter durability. Another function of nanoparticles may consist of long-time conservation of hot electrons injected from the emitter bulk – not only at the bottom of the conductance band (as, for instance, it takes place in diamond), but practically at any energy levels. Hence, the property of low affinity is not necessary for nanostructured emitters to become low-voltage ones, and nanoparticles of sp^2 carbon can facilitate emission as well as the diamond particles. The former may even be preferable, because the broad band gap (in diamond) can hamper the process of generating hot electrons at tunnel junctions if the potential difference between the adjacent grains is not large enough (Fig. 6).

5. Conclusions

The performed investigation of the emission properties of nanoporous carbon has demonstrated that the materials of this type are capable of low-field electron emission. Their emission properties show relatively weak dependency on structural details determined by the technology of their fabrication, e.g. on the combination of the nature of the initial carbide and the temperature of its chemical treatment. Among all the NPC samples ever tested, the only exclusion made those produced from SiC in chlorination process performed at the

highest temperature (2000 °C). These samples lost their nano-scale structure and produced no emission current in the investigated range of the field magnitudes. We explain the obtained results in terms of the two-stage emission model [39,40,61]. We think that 20–200 nm graphitic particles observed at the surface of NPC samples can play the main role in the emission mechanism in two ways: (1) determining substantial enhancement of applied electric field at junctions separating them from the rest of the emitter bulk and (2) providing conditions for conserving non-equilibrium energy distribution of electrons injected into such particles through these junctions.

Acknowledgment

The work was partially supported by the Russian Ministry of Science and Education (grant no. 11.G34.31.0041).

References

[1] N.S. Xu, S. Ejaz Huq, Novel cold cathode materials and applications, Mater. Sci. Eng. R 48 (2−5) (2005) 47–189.
[2] A.N. Obraztsov, Vacuum electronic applications of nano-carbon materials, in: S. Guceri, Yu. G. Gogotsi, V. Kuznetsov (Eds.), Nanoengineered Nanofibrous Materials, Kluwer Academic Publishers, Dordrecht, Boston, London, 2004, pp. 329–339.
[3] A.V. Eletskii, Carbon nanotube-based electron field emitters, Phys. Usp. 180 (9) (2010) 897–930.
[4] K.B.K. Teo, E. Minoux, L. Hudanski, F. Peauger, J.-P. Schnell, L. Gangloff, P. Legagneux, D. Dieumegard, G.A.J. Amaratunga, W.I. Milne, Microwave devices: carbon nanotubes as cold cathodes, Nature 437 (7061) (2005) 968.
[5] M. Dispenza, F. Brunetti, C.-S. Cojocaru, A. de Rossi, A. Di Carlo, D. Dolfi, A. Durand, A.M. Fiorello, A. Gohier, P. Guiset, M. Kotiranta, V. Krozer, P. Legagneux, R. Marchesin, S. Megtert, F. Bouamrane, M. Mineo, C. Paoloni, K. Pham, J.P. Schnell, A. Secchi, E. Tamburri, M.L. Terranova, G. Ulisse, V. Zhurbenko, Towards a THz backward wave amplifier in European OPTHER project, Proc. SPIE 7837 (2010) 783706.
[6] J.X. Huang, J. Chen, J.C. Deng, S.Z. She, N.S. Xu, Field-emission fluorescent lamp using carbon nanotubes on a wire-type cold cathode and a reflecting anode, J. Vac. Sci. Technol. B 26 (2008) 1700–1704.
[7] Z. Li Tolt, C. Mckenzie, R. Espinosa, S. Snyder, M. Munson, Carbon nanotube cold cathodes for application in low current x-ray tubes, J. Vac. Sci. Technol. B 26 (2008) 706–710.
[8] S. Wang, X. Calderon, R. Peng, E.C. Schreiber, O. Zhou, S.A. Chang, Carbon nanotube field emission multipixel x-ray array source for microradiotherapy application, Appl. Phys. Lett. 98 (2011) 213701.
[9] Q. Zou, M.Z. Wang, Y.L. Yang, Field emission from multiwall carbon nanotubes in gas for producing microplasma discharge, J. Appl. Phys. 106 (2009) 013305.
[10] I. Kronhaus, A. Kapulkin, M. Guelman, Field emission cathode with electron optics for use in Hall thrusters, J. Appl. Phys 108 (2010) 054507.
[11] S. Natarajan, C.B. Parker, J.T. Glass, J.R. Piascik, K.H. Gilchrist, C.A. Bower, B.R. Stone, High voltage microelectromechanical systems platform for fully integrated, on-chip, vacuum electronic devices, Appl. Phys. Lett 92 (2008) 224101.
[12] H. Manohara, W.L. Dang, P.H. Siegel, M. Hoenk, A. Husain, A. Scherer, Field emission testing of carbon nanotubes for THz frequency vacuum microtube sources, Proc. SPIE 5343 (2004) 227–234.
[13] I.M. Choi, S.Y. Woo, H.W. Song, Improved metrological characteristics of a carbon-nanotube-based ionization gauge, Appl. Phys. Lett. 90 (2007) 023107.
[14] C.-W. Baik, J. Lee, J.H. Choi, I. Jung, H.R. Choi, Y.W. Jin, J.M. Kim, Structural degradation mechanism of multiwalled carbon nanotubes in electrically treated field emission, Appl. Phys. Lett. 96 (2010) 023105.
[15] X.H. Liang, S.Z. Deng, N.S. Xu, J. Chen, N.Y. Huang, J.C. She, Noncatastrophic and catastrophic vacuum breakdowns of carbon nanotube film under direct current conditions, J. Appl. Phys 101 (2007) 063309.
[16] G.S. Bocharov, A.V. Eletskii, Degradation of a CNT-based field emission cathode due to ion sputtering, Fullerenes Nanotubes Carbon Nanostuct. 20 (2012) 444–450.
[17] S.A. Getty, O. Auciello, A.V. Sumant, X. Wang, D.P. Glavin, P.R. Mahaffy, Characterization of nitrogen-incorporated ultrananocrystalline diamond as a robust cold cathode material, Proc. SPIE 7679 (2010) 76791N.
[18] K. Nose, R. Fujita, M. Kamiko, Y. Mitsuda, Electron field emission from undoped polycrystalline diamond particles synthesized by microwave-plasma chemical vapor deposition, J. Vac. Sci. Technol. B 30 (2012) 011204.
[19] M. Tordjman, A. Bolker, C. Saguy, R. Kalish, Temperature dependence of reversible switch-memory in electron field emission from ultrananocrystalline diamond, Appl. Phys. Lett. 101 (2012) 173116.
[20] J.D. Jarvis, H.L. Andrews, B. Ivanov, C.L. Stewart, N. de Jonge, E.C. Heeres, W.-P. Kang, Y.-M. Wong, J.L. Davidson, C.A. Brau, Resonant tunneling and extreme brightness from diamond field emitters and carbon nanotubes, J. Appl. Phys. 108 (2010) 094322.
[21] C.X. Zhai, J.N. Yun, L.L. Zhao, Z.Y. Zhang, X.W. Wang, Y.Y. Chen, Effect of annealing on field emission properties of nanodiamond coating, Physica B 406 (2011) 1124–1128.
[22] H.F. Cheng, C.C. Horng, H.Y. Chiang, H.C. Chen, I.N. Lin, Modification on the microstructure of ultrananocrystalline diamond films for enhancing their electron field emission properties via a two-step microwave plasma enhanced chemical vapor deposition process, J. Phys. Chem. C 115 (2011) 13894–13900.
[23] K. Uppireddi, B.R. Weiner, G. Morell, Study of the temporal current stability of field-emitted electrons from ultrananocrystalline diamond films, J. Appl. Phys. 103 (2008) 104315.
[24] H. Yamaguchi, T. Masuzawa, S. Nozue, Y. Kudo, I. Saito, J. Koe, M. Kudo, T. Yamada, Y. Takakuwa, K. Okano, Electron emission from conduction band of diamond with negative electron affinity, Phys. Rev. B 80 (2009) 165321.
[25] T. Masuzawa, Y. Sato, Y. Kudo, I. Saito, T. Yamada, A.T.T. Koh, D.H.C. Chua, T. Yoshino, W.J. Chun, S. Yamasaki, K. Okano, Correlation between low threshold emission and C–N bond in nitrogen-doped diamond films, J. Vac. Sci. Technol. B 29 (2011) 02B119.

[26] A.T.T. Koh, Y.M. Foong, J. Yu, D.H.C. Chua, A.T.S. Wee, Y. Kudo, K. Okano, Understanding tube-like electron emission from nanographite clustered films, J. Appl. Phys. 110 (2011) 034903.
[27] V.A. Krivchenko, A.A. Pilevsky, A.T. Rakhimov, B.V. Seleznev, N.V. Suetin, M.A. Timofeyev, A.V. Bespalov, O.L. Golikova, Nanocrystalline graphite: promising material for high current field emission cathodes, J. Appl. Phys. 107 (2010) 014315.
[28] H.H. Busta, R.J. Espinosa, A.T. Rakhimov, N.V. Suetin, M.A. Timofeyev, P. Bressler, M. Schramme, J.R. Fields, M.E. Kordesch, A. Silzars, Performance of nanocrystalline graphite field emitters, Solid-State Electron. 45 (2001) 1039–1047.
[29] O.S. Panwar, M.A. Khan, B.S. Satyanarayana, R. Bhattacharyya, B.R. Mehta, S. Kumar, Effect of high substrate bias and hydrogen and nitrogen incorporation on density of states and field-emission threshold in tetrahedral amorphous carbon films, J. Vac. Sci. Technol. B 28 (2010) 411–422.
[30] L. Xu, C. Wang, C.Q. Hu, Z.D. Zhao, W.X. Yu, W.T. Zheng, Field electron emission enhancement of amorphous carbon through a niobium carbide buffer layer, J. Appl. Phys. 105 (2009) 014302.
[31] J.D. Carey, S.R.P. Silva, Field emission from amorphous semiconductors, Solid-State Electron. 45 (2001) 1017–1024.
[32] A.V. Karabutov, V.D. Frolov, V.I. Konov, V.G. Ralchenko, S.K. Gordeev, P.I. Belobrov, Low-field electron emission of diamond/pyrocarbon composites, J. Vac. Sci. Technol. B 19 (2001) 965–970.
[33] S.F. Ahmed, M.W. Moon, K.R. Lee, Enhancement of electron field emission property with silver incorporation into diamondlike carbon matrix, Appl. Phys. Lett. 92 (2008) 193502.
[34] Y. Zhao, B. Zhang, N. Yao, G. Sun, J. Li, Improved field emission properties from metal-coated diamond films, Diamond Relat. Mater. 16 (2007) 650–653.
[35] K. Uppireddi, B.R. Weiner, G. Morell, Field emission stability and properties of simultaneously grown microcrystalline diamond and carbon nanostructure films, J. Vac. Sci. Technol. B 28 (2010) 1202–1205.
[36] P.C. Huang, W.C. Shih, H.C. Chen, I.N. Lin, The induction of a graphite-like phase on diamond films by a Fe-coating/post-annealing process to improve their electron field emission properties, J. Appl. Phys. 109 (2011) 084309.
[37] K.V. Reich, E.D. Eidelman, A. Ya, Vul', Determination of temperature difference in carbon nanostructures in field emission, Tech. Phys 77 (7) (2007) 123–126.
[38] A. Ilie, A.J. Hart, A. Flewitt, J. Robertson, W.I. Milne, Effect of work function and surface microstructure on field emission of tetrahedral amorphous carbon, J. Appl. Phys. 88 (2000) 6002–6010.
[39] R.G. Forbes, Low-macroscopic-field electron emission from carbon films and other electrically nanostructured heterogeneous materials: hypotheses about emission mechanism, Solid-State Electron. 45 (2001) 779–808.
[40] J.D. Carey, S.R.P. Silva, Disorder, clustering, and localization effects in amorphous carbon, Phys. Rev. B 70 (2004) 235417.
[41] M.W. Geis, N.N. Efremow, K.E. Krohn, J.C. Twichell, T.M. Lyszczarz, R. Kalish, J.A. Greer, M.D. Tabat, A new surface electron-emission mechanism in diamond cathodes, Nature 393 (1998) 431–435.
[42] S.R.P. Silva, G.A.J. Amaratunga, K. Okano, Modeling of the electron field emission process in polycrystalline diamond and diamond-like carbon thin films, J. Vac. Sci. Technol. B 17 (1999) 557–561.
[43] X. Shi, L.K. Cheah, B.K. Tay, S.R.P. Silva, Electron field emission from surface treated tetrahedral amorphous carbon films, Appl. Phys. Lett. 74 (1999) 833–835.
[44] A.N. Obraztsov, A.A. Zakhidov, Low-field electron emission from nano-carbons, Diamond Relat. Mater. 13 (2004) 1044–1049.
[45] I.S. Altman, P.V. Pikhitsa, M. Choi, Two-process model of electron field emission from nanocarbons: temperature effect, J. Appl. Phys. 96 (2004) 3491–3493.
[46] S. Gupta, B.R. Morell, G. Weiner, Electron field-emission mechanism in nanostructured carbon films: a quest, J. Appl. Phys. 95 (2004) 8314–8320.
[47] W.G. Xie, Jun Chen, Jian Chen, S.Z. Deng, J.C. She, N.S. Xu., Effect of hydrogen treatment on the field emission of amorphous carbon film, J. Appl. Phys. 101 (2007) 084315.
[48] S.H. Lai, K.L. Chang, H.C. Shih, K.P. Huang, P. Lin, Electron field emission from various morphologies of fluorinated amorphous carbon nanostructures, Appl. Phys. Lett. 85 (2004) 6248–6250.
[49] M. Ojima, S. Hiwatashi, H. Araki, A. Fujii, M. Ozaki, K. Yoshino, Pore size dependence of field emission from nanoscale porous carbon, Appl. Phys. Lett. 88 (2006) 053103.
[50] E. Smorgonskaya, R. Kyutt, A. Danishevskii, C. Jardin, R. Meaudre, O. Marty, S. Gordeev, A. Grechinskaya, X-ray and HRTEM structural studies of bulk nanoporous carbon materials produced from carbides, J. Non-Cryst. Solids 299–302 (2) (2002) 810–814.
[51] A.I. Veinger, B.D. Shanina, A.M. Danishevskii, V.V. Popov, S.K. Gordeev, A.V. Grechinskaya, Electrophysical studies of nanoporous carbon materials prepared of silicon carbide powders, Sov. Phys. – Solid State 45 (6) (2003) 1141–1150.
[52] E.N. Hoffman, G. Yushin, M.W. Barsoum, Y. Gogotsi, Synthesis of carbide-derived carbon by chlorination of Ti2AlC, Chem. Mater. 17 (2005) 2317–2322.
[53] A.E. Kravchik, Ju.A. Kukushkina, V.V. Sokolov, G.F. Tereshchenko, Structure of nanoporous carbon produced from boron carbide, Carbon 44 (2006) 3263–3268.
[54] A.E. Kravchik, Ju.A. Kukushkina, V.V. Sokolov, G.F. Tereshchenko, E.A. Ustinov, Structure of nanoporous carbon produced from titanium carbide and carbonitride, Russ. J. Appl. Chem. 81 (10) (2008) 1605–1612.
[55] A. Arkhipov, S. Davydov, P. Gabdullin, N. Gnuchev, A. Kravchik, S. Krel, Field-induced electron emission from nanoporous carbons, J. Nanomater. 2014 (2014) 190232.
[56] V.B. Bondarenko, P.G. Gabdullin, N.M. Gnuchev, S.N. Davydov, V.V. Korablev, A.E. Kravchik, V.V. Sokolov, Emissivity of powders prepared from nanoporous carbon, Tech. Phys. 74 (10) (2004) 113–116.
[57] O. Groening, L.-O. Nilsson, P. Groening, L. Schlapbach, Properties and characterization of chemical vapor deposition diamond field emitters, Solid-State Electron. 45 (6) (2001) 929–944.
[58] A.A. Zakhidov, A.N. Obraztsov, A.P. Volkov, D.A. Lyashenko, Statistical analysis of low-voltage electron emission from nanocarbon cathodes, J. Exp. Theor. Phys. 97 (6) (2003) 1240–1245.

[59] N. Koenigsfeld, R. Kalish, A. Hoffman, Improved field emission at electric-discharge-conditioned sites on diamond surfaces due to the formation of carbon nanotubes, Appl. Phys. Lett. 82 (26) (2003) 4687–4689.
[60] A.Yu. Babenko, A.T. Dideykin, E.D. Eidelman, Graphene ladder: a model of field emission center on the surface of loose nanocarbon materials, Phys. Solid State 51 (2) (2009) 410–414.
[61] A.V. Arkhipov, M.V. Mishin, I.V. Parygin, Hysteresis of pulsed characteristics of field emission from nano-carbon materials, Surf. Interface Anal. 39 (2007) 149–154.
[62] S.N. Davydov, P.G. Gabdullin, M.A. Ryumin, Apparatus for investigating physical nature of nanoporous carbon structure field emission, in: Proceedings of the Abstracts of International Workshop on Fullerenes and Atomic Clusters, 6–10 July 2009, St. Petersburg, Russia, A. F. Ioffe Institute, St. Petersburg, Russia, 2009, p. 165.
[63] A.V. Arkhipov, P.G. Gabdullin, M.V. Mishin, On possible structure of field-induced electron emission centers of nanoporous carbon, Fullerenes Nanotubes Carbon Nanostruct. 19 (2011) 86–91.
[64] G.C. Kokkorakis, J.P. Xanthakis, Local electric field and enhancement factor around nanographitic structures embedded in amorphous carbon, Surf. Interface Anal. 39 (2007) 135–138.
[65] A. Pandey, P. Guyot-Sionnest, Hot electron extraction from colloidal quantum dots, Science 322 (2008) 929–932.
[66] W.A. Tisdale, K.J. Williams, B.A. Timp, D.J. Norris, E.S. Aydil, X.Y. Zhu, Hot-electron transfer from semiconductor nanocrystals, Science 328 (2010) 1543–1547.
[67] H. Benisty, Reduced electron-phonon relaxation rates in quantum-box systems: theoretical analysis, Phys. Rev. B 51 (1995) 13281–13293.
[68] T. Inoshita, H. Sakaki, Electron-phonon interaction and the so-called phonon bottleneck effect in semiconductor quantum dots, Physica B 227 (1996) 373–377.
[69] A.J. Nozik, Spectroscopy and hot electron relaxation dynamics in semiconductor quantum wells and quantum dots, Annu. Rev. Phys. Chem. 52 (2001) 193–231.
[70] K. Mukai, M. Sugawara, Phonon bottleneck effect in quantum dots, in: Self-Assembled InGaAs/GaAs Quantum Dots, vol. 60, Academic Press, San Diego, 1999, p. 209.